THE EXPRESSION OF THE INTERMEDIATE FILAMENTS GLIAL FIBRILLARY ACIDIC PROTEIN AND KERATIN IN THE VISUAL PATHWAY OF *DANIO RERIO*

Approved:

_____
Dr. Heather C. Galloway
Director, University Honors Program

Approved:

_____
Dr. Joseph R. Koke
Department of Biology
Supervising Professor

THE EXPRESSION OF THE INTERMEDIATE FILAMENTS GLIAL FIBRILLARY ACIDIC PROTEIN AND KERATIN IN THE VISUAL PATHWAY OF *DANIO RERIO*

HONORS THESIS

Presented to the Honors Committee of

Texas State University-San Marcos

In Partial Fulfillment of

the Requirements

For Graduation in the University Honors Program

By

Kyle Joseph Henry

San Marcos, Texas

May 2009

ACKNOWLEDGEMENTS

I would like to thank Dr. Koke for his guidance and patience throughout this experiment. I also would to express my gratitude to Mya Patel and Elizabeth Capalbo, Graduate Students of the Koke and García Labs, for their advice, instruction, and vigilant reminders of lab etiquette.

This work was supported in part by National Science Foundation MRI grant to JK and DG #DBI-0821252 and a Faculty Research Enhancement Award to JK.

Dedicated to my parents – constant inspirations and those responsible for making me the person I am today.

ABSTRACT

There is some debate in zebrafish literature in regards of what type of intermediate filament (IF) is expressed in astrocytes of zebrafish optic nerve. Some research groups claim glial fibrillary acidic protein (GFAP) is prominent. Others argue cytokeratin is expressed, but not GFAP. Using Immuno histochemistry, GFAP and cytokeratins present in the zebrafish visual pathway were identified. Purified mouse monoclonal antibodies against GFAP and cytokeratin 18 were used in combination with goat anti-mouse IgG antibodies conjugated to Rhodamine Red-X and Alexa Fluor 488, respectively, to identify the IFs found in the zebrafish visual pathway. Observations of immuhistochemically stained tissues under an Olyumpus Fluoview FV1000 confirmed the presence of cytokeratin in the zebrafish optic nerve, but did not present evidence confirming or denying the presence of GFAP in the zebrafish optic nerve.

INTRODUCTION

There has been some debate as to which intermediate filaments (IFs) are expressed in the optic nerve of *Danio rerio* (zebrafish). Most literature suggests glial fibrillary acidic protein (GFAP) is restricted to astrocytes of retina, brainstem, and spinal cord in uninjured fish (Nona et al. 1989) while others suggest it may be expressed in the optic nerve as well (Cohen et al. 1993). The other IFs of interest in this experiment are keratins. Keratins are generally found in epithelial cells and their derivatives and are considered prominent in the optic nerve (Herrmann and Harris. 1998).

Zebrafish are model vertebrates for studying the central nervous system (CNS) because the zebrafish genome has been completed, they are inexpensive, and are easily maintained. The zebrafish brain also contains relatively few neurons and glial cells and its neuronal network therefore can be easily analyzed (Kawai et al. 2001). Zebrafish have also shown impressive nerve regeneration capabilities, which have led to their extensive use in CNS studies (García and Koke, 2008). Successful identification of the IFs found in the zebrafish optic nerve will clarify the cytoskeletal structure of those cells found in the uninjured optic nerve, which will aid further research of the zebrafish visual pathway. Proper identification of the location of cytokeratins and GFAP in uninjured fish will also have ramifications for the amount of GFAP observed in the optic nerve during neurogenesis after an optic nerve injury.

Intermediate filaments (IFs) are ubiquitous cytoskeleton scaffolding found in the nucleus and cytoplasm of higher metazoans (Erber et al. 1998). The main proposed function of IFs is to provide cells with resistance to mechanical stress caused by external forces or internal processes, such as cell division or migration (Goldman et al., 1996). IFs self-

assemble from fibrous, elongated coiled-coil dimers (Parry and Steiner, 1999. and Aebi et al., 1988). The elementary IF dimer includes a central coiled-coil “rod” domain containing close to 300 residues and non-alpha-helical N- and C-terminal end domains (Strelkov et al. 2002). According to their amino acid sequence, six IF protein types are generally distinguished: types I and II (keratins), type III (vimentin, desmin, GFAP, peripherin, and plasticin), type IV (neurofilament proteins, alpha internexin, gelfiltin, and xefiltin), type V (nuclear lamins), and the heterogeneous type VI (including nestin, synemin, paranemin, syncoilin, and tanabin) (García et al. 2005). GFAP is most commonly associated with astrocytes, as well as some ependymal cells, and is important in neurogenesis and gliogenesis (Menet et al. 2000). Astrocytes belong to a family of neuroglial cells and are important in neurogenesis and gliogenesis (Maeyama and Nakayasu. 2000). There have been 16 type I, and 7 type II keratins identified in the zebrafish genome (Padhi, et al. 2006). As stated before, cytokeratins form complex networks essential for the structural integrity of epithelial cells (Alberts et al. 2007), and are prominent in the optic nerve (Herrmann and Harris. 1998).

Immunohistochemisty (IHC) is the practice of labeling biological molecules via the binding of antibody to antigen present in biological tissue. Typically, a primary antibody is used to identify an antigen in a specific protein, and a secondary antibody, conjugated to a fluorescent agent, recognizes the primary antibody. The secondary antibody can be observed under an epifluorescent microscope as a fluorescent signal at a particular wavelength of light. This fluorescence essentially identifies the protein the primary antibody is bound to. Antibodies can be monoclonal or polyclonal. Monoclonal antibodies are antibodies produced by a single B-cell clone, and are thus identical. Polyclonal antibodies are produced by plasma cells in response to different features, or epitopes, of an antigen, which can result in many

different antibodies directed to the same antigen. Monoclonal antibodies are more specific but have less avidity. They will identify the epitope they were developed against, and usually show little or know cross reactivity among antigens. Polyclonal antibodies have higher avidity and tend to be more cross-reactive, as they recognize epitopes that may appear on more than one antigen (Lipman et al. 2005).

MATERIALS AND METHODS

Fish Maintenance

Wild-type zebrafish were obtained from a local pet store (Animal Wonders, San Marcos), which were originally from obtained from Scientific Hatcheries, now located in Aquatic Tropicals, Florida. All protocols were approved by the Texas State IACUC (approval #0703_0122_07).

Chemicals

All chemicals were of reagent grade and prepared at Texas State Univeristy-San Marcos unless otherwise noted. Paraformaldehyde (PFA) was from Electron Microscopy Sciences (Fort Washington, PA). Sucrose, sodium chloride, and triton-X-100 were from Sigma (St. Louis MO). Tris was from Bio-Rad laboratories (Hercules, CA). Sodium phosphate was from Fisher Chemicals (Fairtown, NJ). Potassium chloride and dibasic potassium phosphate were from EM Science (Gibbstown, NJ). Tricain methylsulfonate (MS-222) was from Finquel (Redmond, WA). The mouse monoclonal anti-GFAP antibody 131-17719, the Hoechst 33342 trihydrochloride trihydrate (H1399), the Alexa Fluor 488 and Rhodamine Red-X Goat anti-mouse IgG antibodies were from Molecular Probes (Eugene, OR). The Anti-KRT18 purified mouse monoclonal antibody was from Abgent (San Diego, CA). Gelatin was obtained from Fisher Scientific (Fair Lawn, NJ). PFA, PBS, and PBST were made at Texas State University (San Marcos, Tx).

Equipment

The cryosection used was an HM505N model from Thermoscientific Microm (Walldorf, Germany). The confocal laser scanning biological microscope was a Fluoview FV1000 from Olympus (Center Valley, PA).

Tissue Preparations

Zebrafish were anesthetized and sacrificed using MS-222. The sacrificed zebrafish were then fixed in 4% PFA overnight at 4℃. The zebrafish were then dissected such that eyes, brain, and optic nerve, fully intact and together, were removed from the rest of the fish. As much connective tissue was removed as possible from the eye, brain, and optic nerve without destroying the tissue, or separating any of the specimen. The fixed eyes, brain, and optic nerve were then washed with phosphate buffered saline (PBS) three times for ten minutes each time, one wash directly following the completion of the previous.

These dissections were placed in 30% sucrose overnight at room temperature for cryoprotection. The dissections were removed from the sucrose solution, and cryosectioned at 14 nm onto 0.5% gelatin coated cover slips such that eye, brain, and optic nerve were together on each section.

Immunohistochemical Staining and Observations

The sections were incubated in 1% PBST for 5 minutes. The PBST was removed, and the sections were incubated in 10% non-fat dry milk for 2 hours. The slides were then washed in 1% PBST three times for ten minutes each wash. The sections were incubated in primary antibody overnight at 4℃. Cytokeratin experimental sections were incubated in 2.5 µg/ml anti-KRT18 purified mouse monoclonal antibody. GFAP experimental sections were incubated in 1.5 µg/ml anti-GFAP purified mouse monoclonal antibody. Controls were incubated in PBS. After the overnight incubation, all sections were washed in PBS three times for ten minutes each wash. The sections were then incubated in secondary antibody at room temperature for two hours. All cytokeratin sections (including controls) were incubated in 20 µg/ml Alexa Fluor 488. All GFAP sections were incubated in 20 µg/ml Rhodamine

Red-X. All sections were again washed in PBS three times for ten minutes each wash. All sections were then incubated in 0.5 μg/ml Hoechst 33342 trihydrochloride trihydrate nuclear stain for fifteen minutes at room temperature. The sections were once again washed in PBS three times for ten minutes each wash. The sections were mounted in 90% glycerol on microscope slides. These slides were observed under an Olympus Fluoview FV1000 confocal laser scanning biological microscope.

RESULTS

Figure 1 is an image of anti-KRT18 labeled optic nerve. The spots of bright fluorescence, as evidence by the intensity profile for the image (Figure 2), indicate the presence of cytokeratin. Figure 3 is another image of anti-KRT labeled optic nerve, and presents the same evidence as Figure 1. Figure 5 is an image of the anti-KRT18 control, which was not incubated in primary antibody. There is some autofluorescence in the image, but it lacks the bright fluorescent labeling observed in Figures 1 and 3. The intensity profile for Figure 5 (Figure 6) does not contain the sharp spikes that provide evidence of brighter labeling like the intensity profiles for Figures 1 and 3 (Figures 2 and 4, respectively). Figure 7 is a three dimensional image of a region of interest of an experimental cytokeratin section. Much of the green observed in the image can be associated with autofluorescence that is also observed in the control sections, Figure 9. Again, the bright labeling is observable in these three-dimensional images as well.. It is important to note the scale of each y-axis on the intensity profiles. These graphs clearly demonstrate the differences in the brightness of the sections.

Figures 11 and 13 are images of experimental and control GFAP sections, respectively. There is obvious labeling in the experimental section, and the control is much more dull in terms of fluorescence, as observed by their intensity profiles (Figures 12 and 13, respectively). There is also, however, intense labeling in regions of the experimental not associated with GFAP, such as muscle tissue and blood vessels. Figure 15 is an image of anti-GFAP labeled zebrafish retina. The labeling of Müller glia projections in this image is indicative that the anti-GFAP antibody is labeling GFAP. The control zebrafish retina image (Figure 18) does not provide any evidence of labeling or autofluorescence.

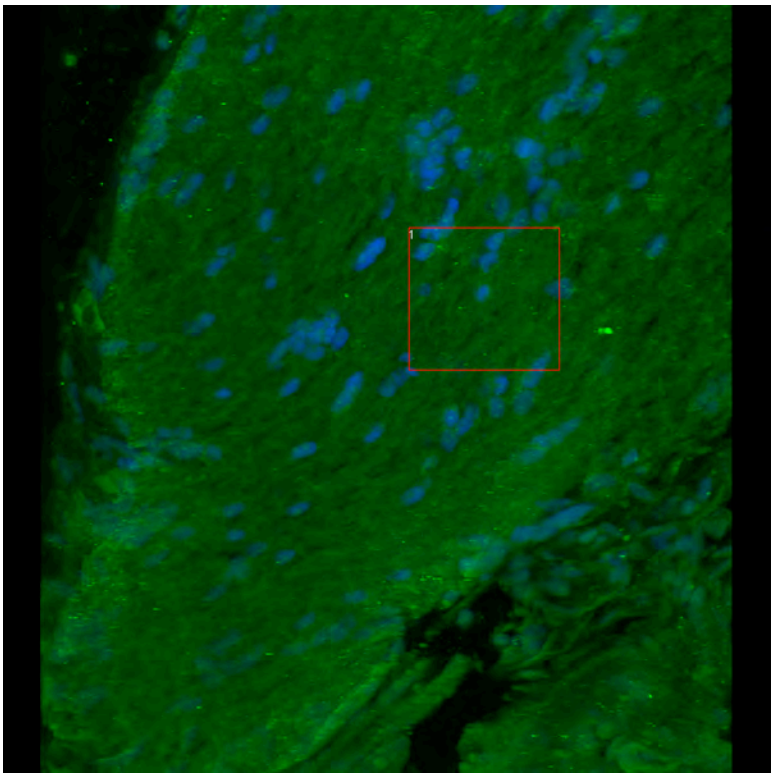

Figure 1. Anti-KRT18 Labels Cytokeratin in the Zebrafish Optic Nerve. This is an image of zebrafish optic nerve stained with 2.5 µg/ml anti-KRT18. The bright spots of fluorescence indicate the presence of cytokeratin, due to the binding of the primary antibody to the IF and the binding of the secondary antibody to the primary. The red square outlines the region of interest of this section. The blue fluorescence is due to a nuclear stain, which labels nuclei.

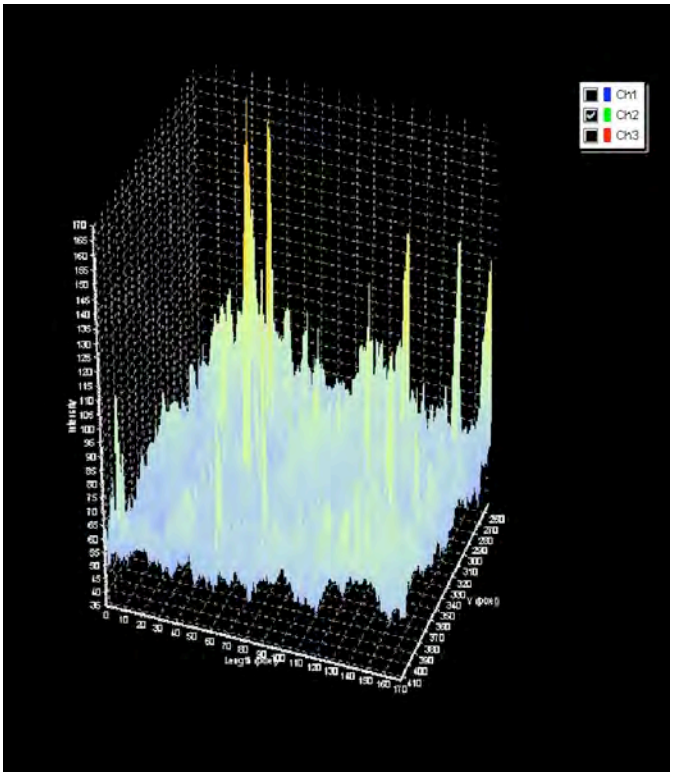

Figure 2. Pixel Intensity Profile of the Region of Interest in Figure 1. This graph demonstrates the pixel intensity of green in the region of interest found in Figure 1. The spikes indicate increased intensity of the pixels associated with the images of fluorescent labeling. The intensity spikes occur at the locations where cytokeratin is labeled. Note the scale of the y-axis.

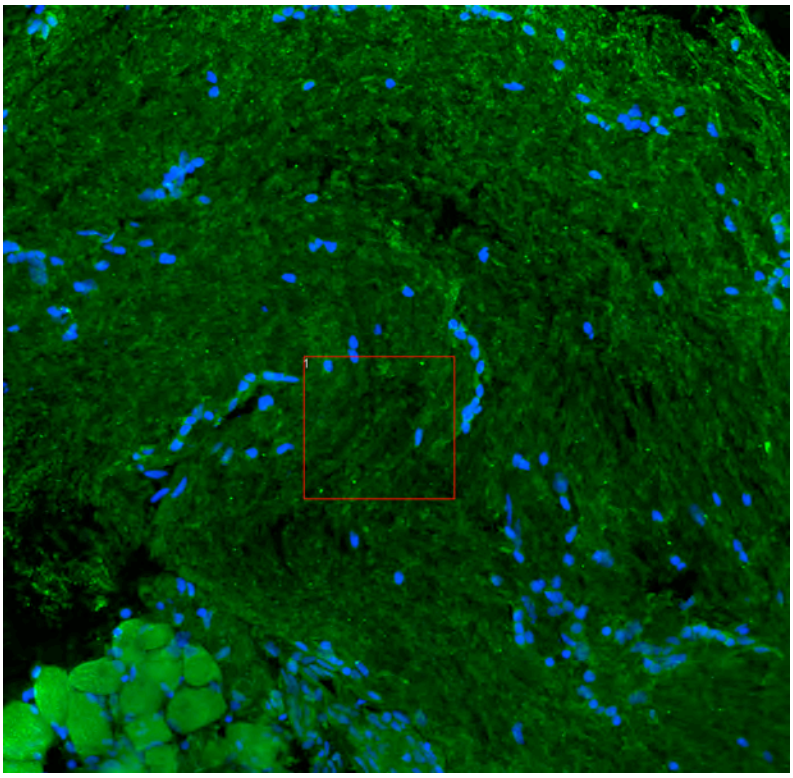

Figure 3. Further Anti-KRT18 Labeling in the Zebrafish Optic Nerve. This is another image of zebrafish optic nerve labeled with 2.5 µg/ml anti-KRT18. The bright spots of fluorescence indicate the presence of cytokeratin, due to the binding of the primary antibody to the IF and the binding of the secondary antibody to the primary. The red square outlines the region of interest of this section.

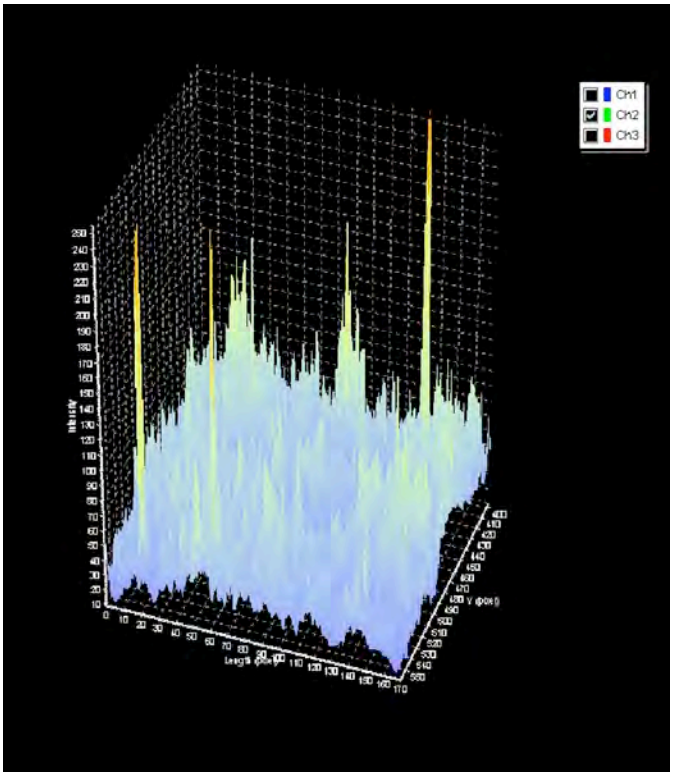

Figure 4. Pixel Intensity Profile of the Region of Interest in Figure 3. This graph demonstrates the pixel intensity of the green in the region of interest found in Figure 3. The spikes indicate increased intensity of the pixels associated with the brightness of fluorescent labeling. The intensity spikes occur at the locations where cytokeratin is labeled. The scale of the y-axis should be noted.

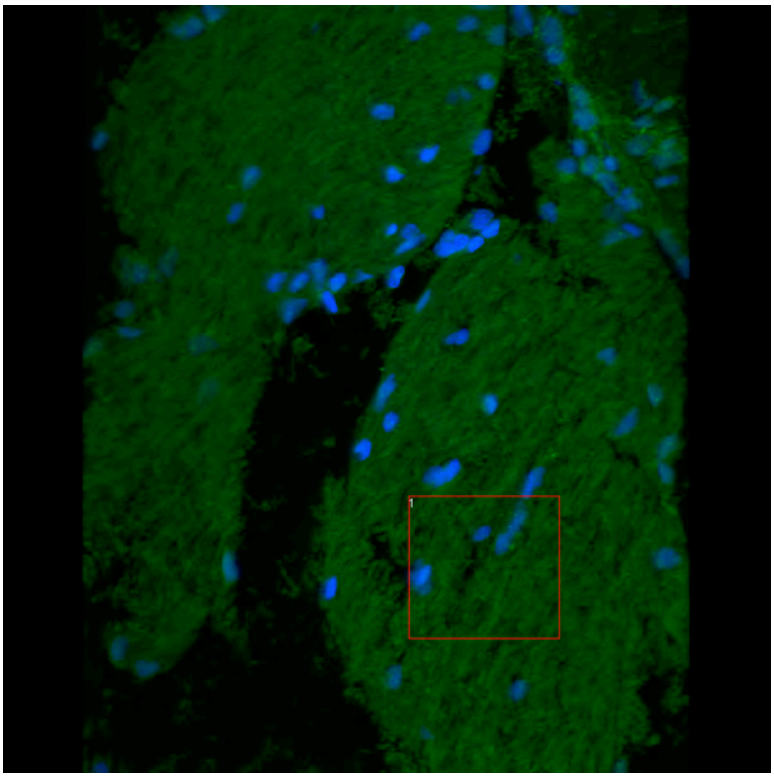

Figure 5. Zebrafish Optic Nerve without Primary Antibody – Anti-KRT18 Control. This image shows a zebrafish optic nerve section without primary antibody. Notice that the bright labeling observed in the experimental sections is not observed. The bright green is simply due to the autofluorescence of lamina in the cells. The region of interest is outlined in red.

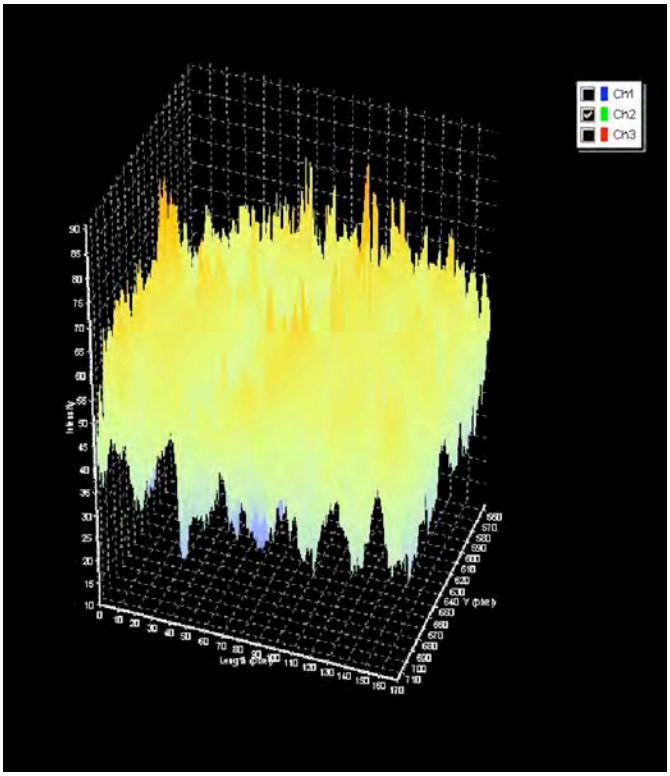

Figure 6. Pixel Intensity Profile of the Region of Interest in Figure 5. This graph demonstrates the pixel intensity of the green in the region of interest found in Figure 5. Notice the differences in the y-axis scale values between intensity profiles of the control and the experimental. This profile is also lacking the discrete spikes observed in the experimental sections.

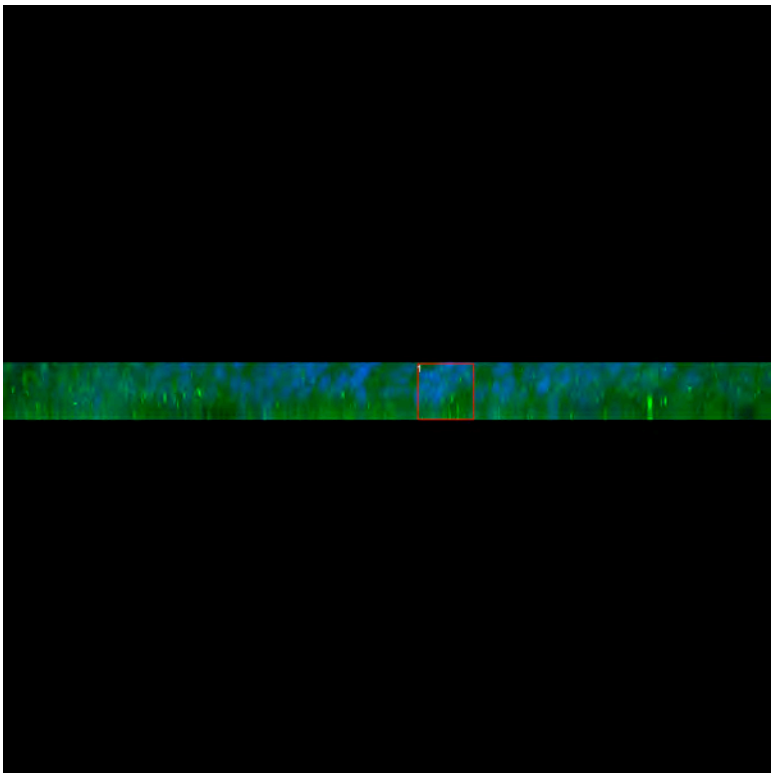

Figure 7. Anti-KRT18 Cytokeratin Labeling of a Horizontal Three-Dimensional Projection of Zebrafish Optic Nerve. This image is a horizontal projection of a stack of images (one of which can be seen in Figure 1) which, when combined, produces a three dimensional representation of the tissue. The fluorescent labeling within the tissue confirms that the labeling is labeling in the tissue and not a precipitate on the surface.

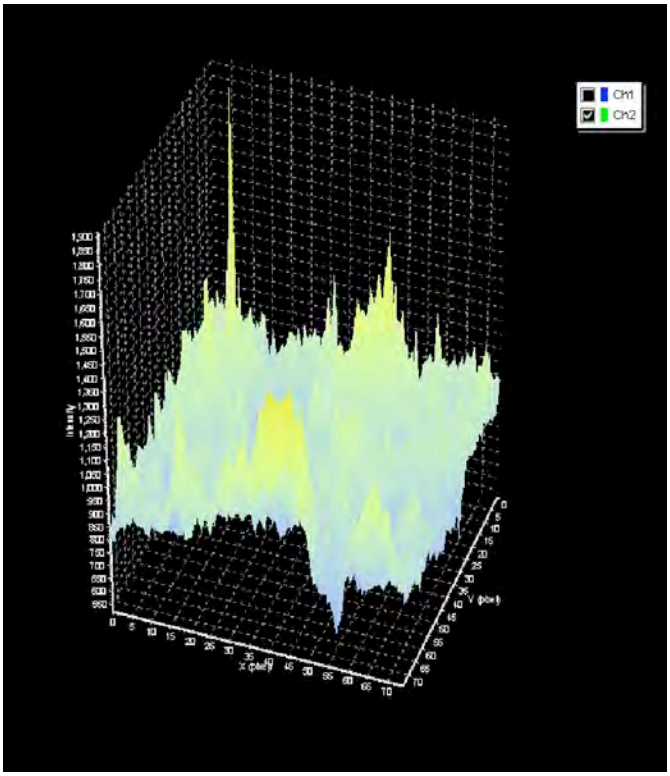

Figure 8. Pixel Intensity Profile of the Region of Interest in Figure 7. This graph demonstrates the pixel intensity of the green in the region of interest found in Figure 7. Because of the depth of this image, the autofluorescence is compounded making the overall intensity of the region of interest greater, but the discrete spikes indicating labeling with the primary antibody and its corresponding fluorescence are still discernable. The scale of the y-axis is much greater in this intensity profile than in the others.

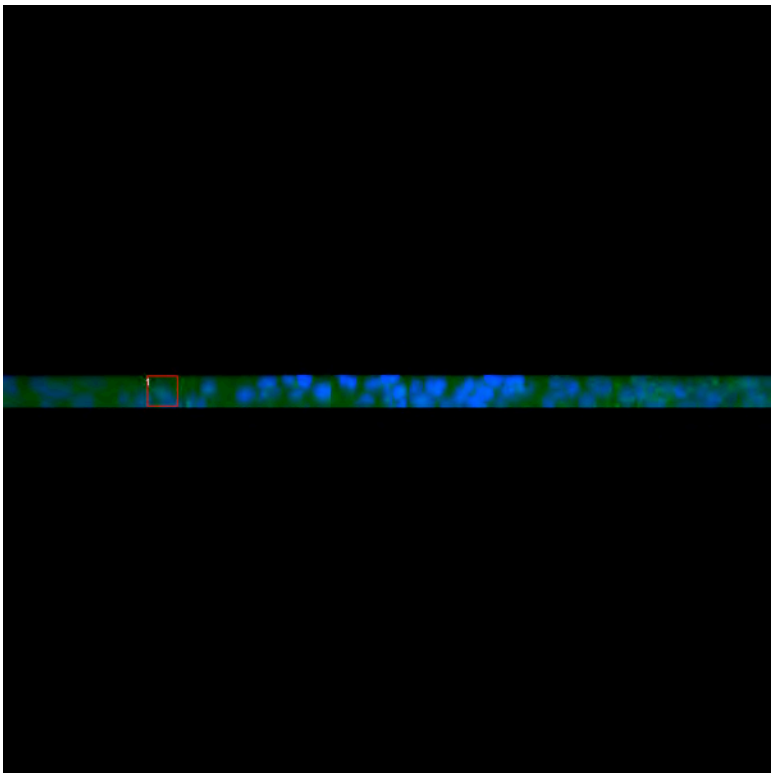

Figure 9. Horizontal Three-Dimensiional Projection of Zebrafish Optic Nerve without Primary Antibody – Anti-KRT18 Control. This image is a horizontal projection of a stack of images (one of which can be seen in Figure 5) of the control tissue, which, when combined, produces a three dimensional representation of the tissue. Bright fluorescent labeling observed in Figure 7 is not present here.

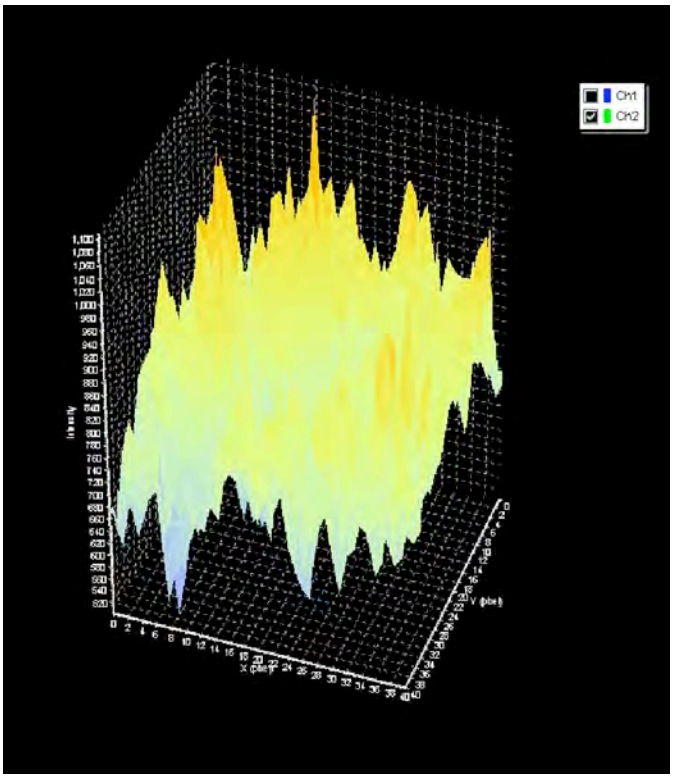

Figure 10. Pixel Intensity Profile of the Region of Interest in Figure 9. This graph demonstrates the pixel intensity of the green in the region of interest found in Figure 9. Notice the differences in the y-axis scale values between intensity profiles of the control and the experimentals. This profile is also lacking the discrete spikes observed in the experimental section.

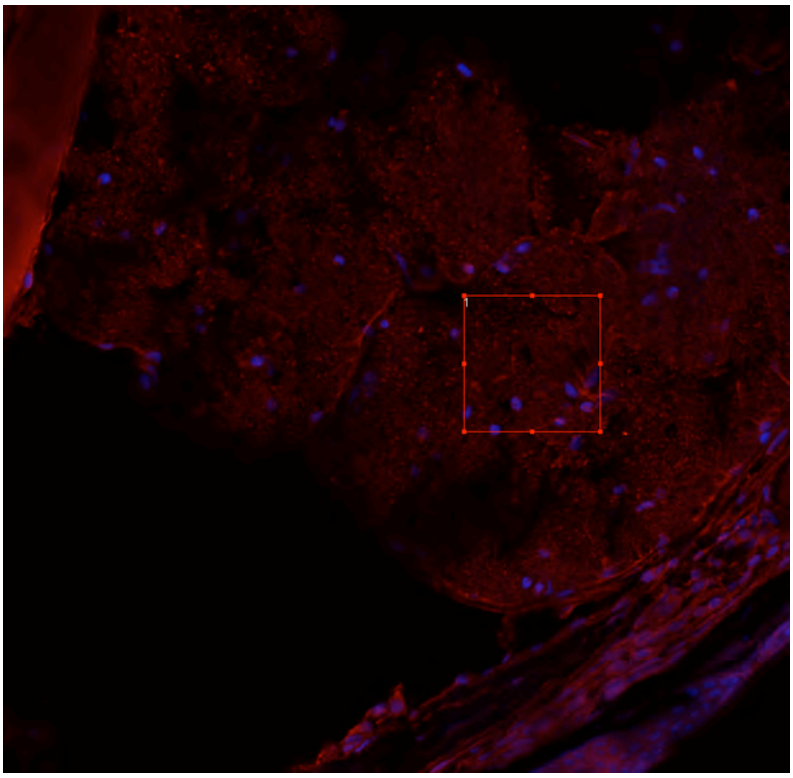

Figure 11. Anti-GFAP Labels IFs in the Zebrafish Optic Nerve. This is an image of zebrafish optic nerve stained with 1.5 µg/ml anti-GFAP. The labeling observed is non-specific, but most likely related to type III IFs. The labeling of muscle tissue (upper left corner) and blood vessels (bottom right corner) provides evidence that the antibody used is non-specific, and therefore the labeling in the optic nerve could be from GFAP or a different IF. The region of interest is outlined in red. Again, the blue fluorescence is due to a nuclear stain, which labels the nuclei.

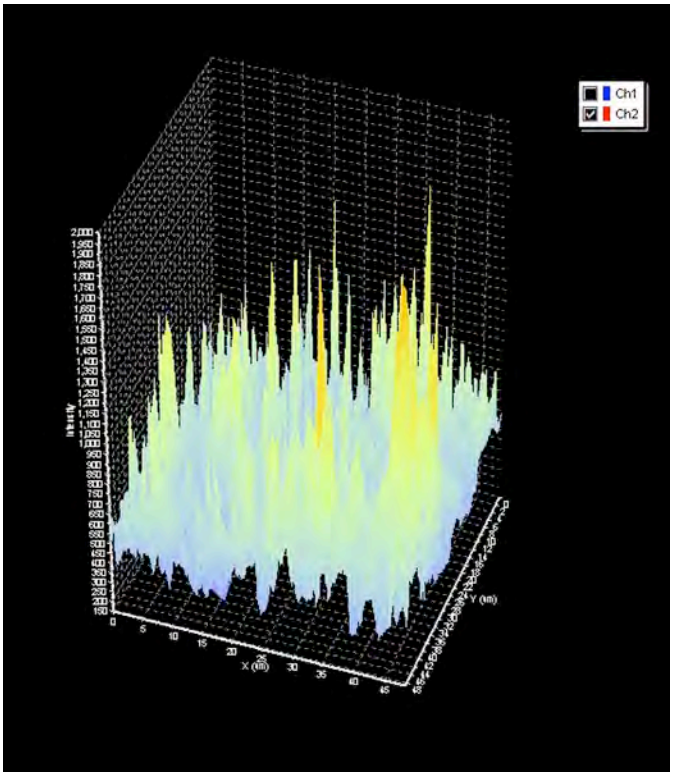

Figure 12. Pixel Intensity Profile of the Region of Interest in Figure 11. This graph demonstrates the pixel intensity of the red in the region of interest found in Figure 11. The sharp spikes indicate fluorescent labeling due to the antibody. Notice the y-axis scale values.

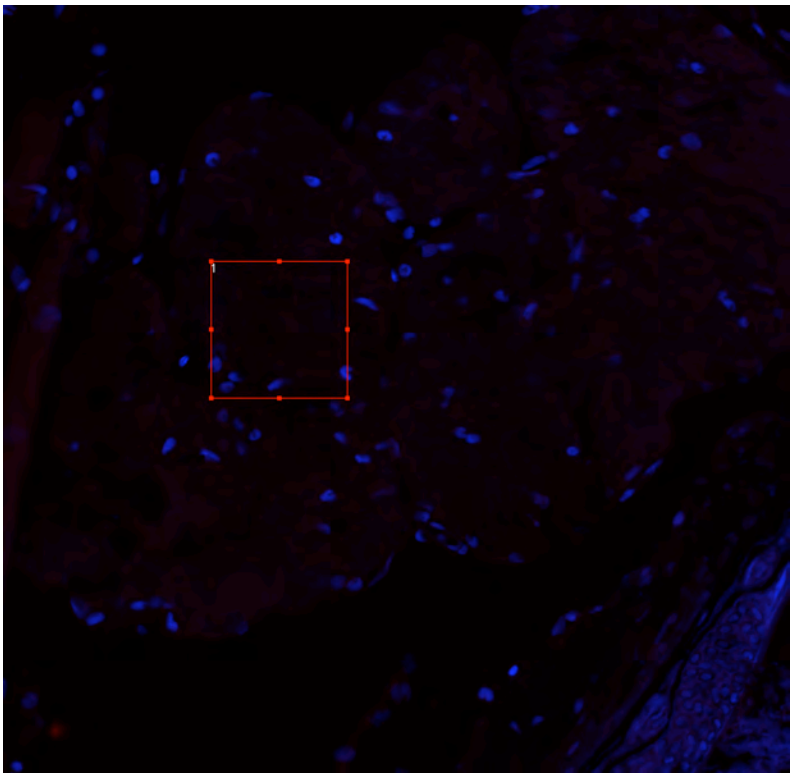

Figure 13. Zebrafish Optic Nerve without Primary Antibody – Anti-GFAP Control. This is an image of zebrafish optic nerve without primary antibody. This is an excellent control, with almost no autofluorescence or labeling due to antibody. The blue fluorescence of the nuclear stain is much more visible than the red of the rest of the cell, but the red is still barely visible. The region of interest is outlined in red.

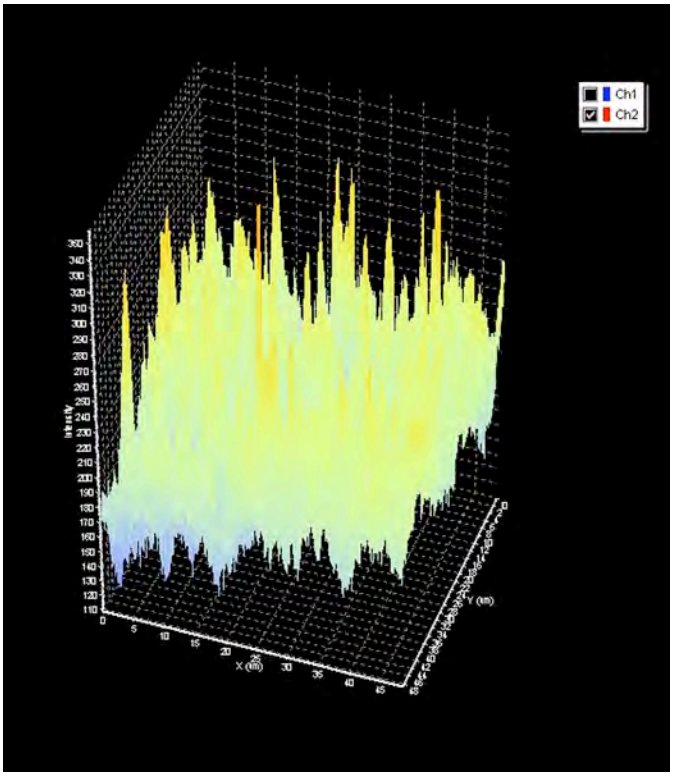

Figure 14. Pixel Intensity Profile of the Region of Interest in Figure 13. This graph demonstrates the pixel intensity of the red in the region of interest found in Figure 13. The very low values of the y-axis scale demonstrate little autofluorescence and no fluorescence due to antibody labeling.

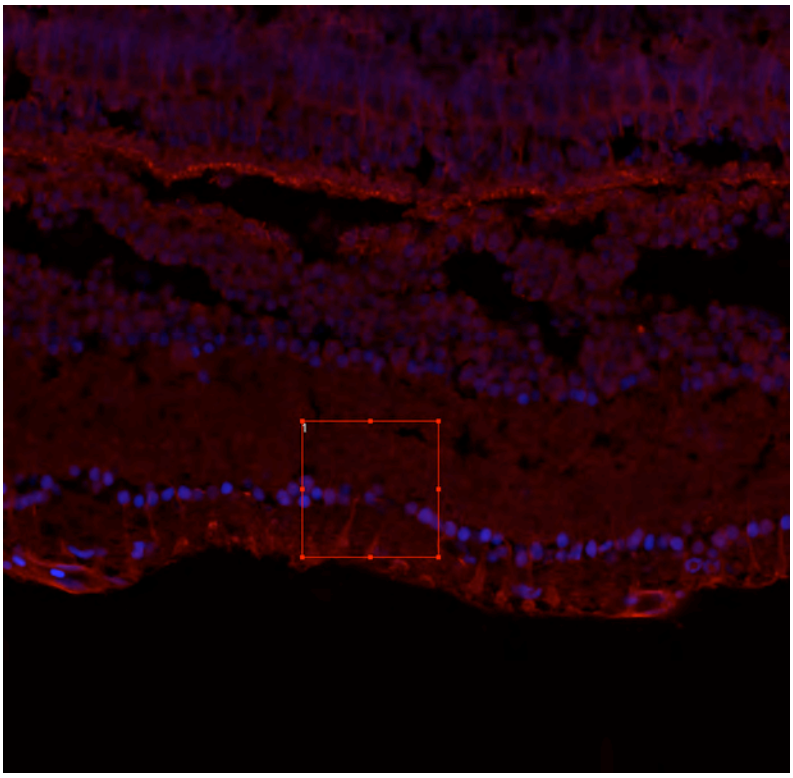

Figure 15. Anti-GFAP Labels IFs in the Zebrafish Retina. This is an image of zebrafish retina stained with 1.5 µg/ml anti-GFAP. The projections at the bottom of the image are most likely Müller glia, a type of astrocyte. These projections give evidence that the anti-GFAP antibody does label GFAP, as well as some other IFs. The blue fluorescence is due to a nuclear stain, which labels the nuclei.

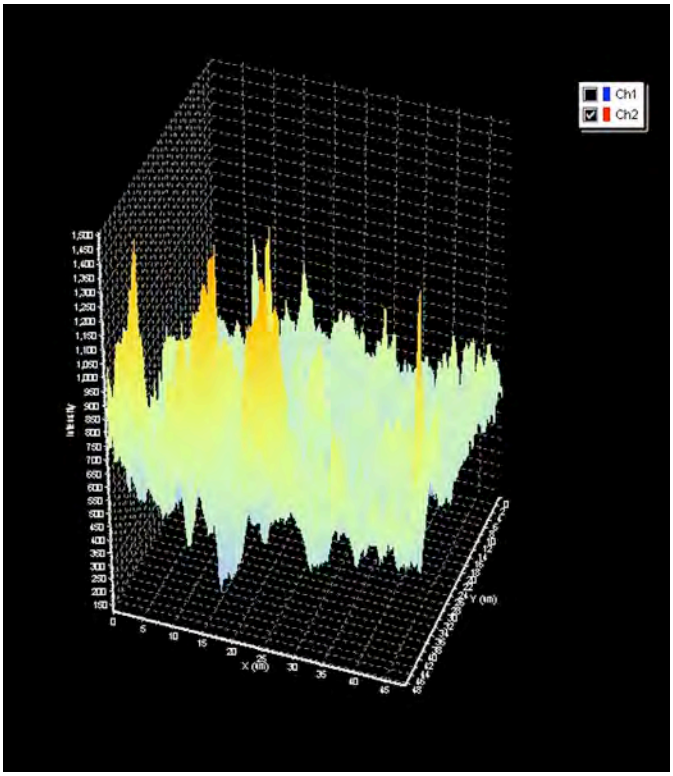

Figure 16. Pixel Intensity Profile of the Region of Interest in Figure 15. This graph demonstrates the pixel intensity of the red in the region of interest found in Figure 15. The sharp spikes indicate fluorescent labeling due to the antibody. Of note is the sharp spikes at the front of the z-axis corresponding to the labeling of the GFAP in the Müller glia projections. Notice the y-axis scale values.

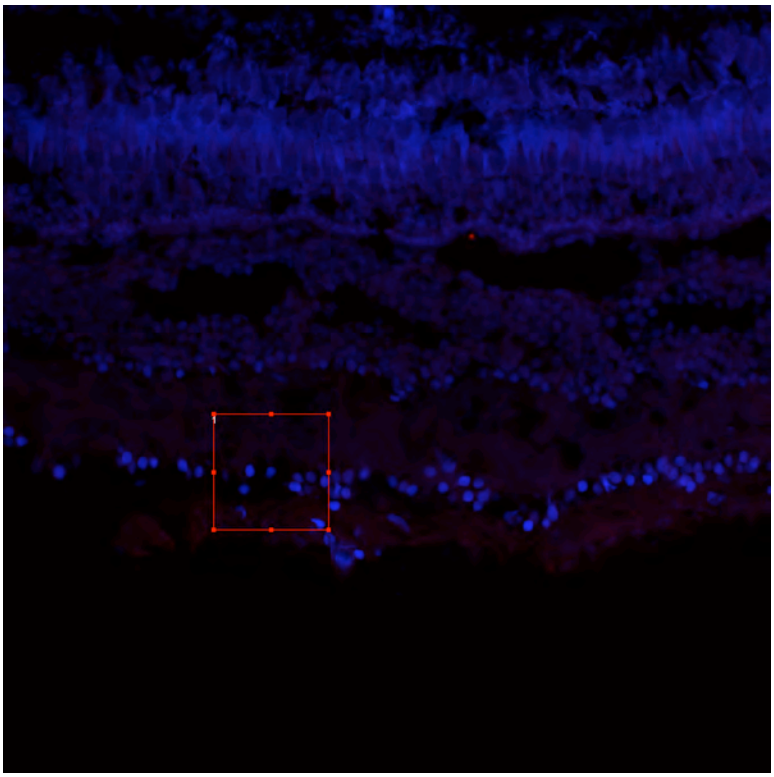

Figure 17. Zebrafish Retina without Primary Antibody – Anti-GFAP Control. This is an image of zebrafish retina without primary antibody. This is an excellent control, with almost no autofluorescence or labeling due to antibody. The blue fluorescence of the nuclear stain is much more visible than the red of the rest of the cell, but the red is still barely visible. The bright blue fluorescence at the top of the image is due to the autofluorescence of photoreceptors. The region of interest is outlined in red.

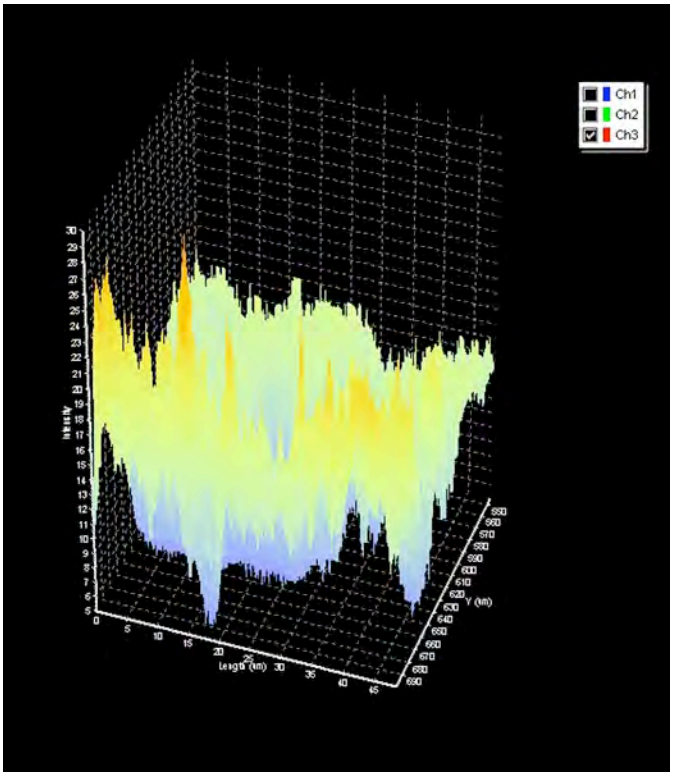

Figure 18. Pixel Intensity Profile of the Region of Interest in Figure 17. This graph demonstrates the pixel intensity of the red in the region of interest found in Figure 17. The very low values of the y-axis demonstrate little autofluorescence and no fluorescence due to antibody labeling.

DISCUSSION

The results of the experiment indicate that cytokeratin is found in the zebrafish optic nerve. The results concerning GFAP in the zebrafish optic nerve are inconclusive.

The bright spots of fluorescence found in the experimental cytokeratin sections are indicative that the anti-KRT18 purified mouse monoclonal antibody has bound to keratin, and the Alexa Fluor 488 goat anti-mouse IgG antibody has bound to the primary antibody. The Alexa Fluor attached to the secondary antibody fluoresces green at those sites where the antibody has bound. The absence of these spots of fluorescence in the control indicates that the green fluorescence in the control sections is simply due to autoflorescence of the cells, and not due to binding of the primary or secondary antibody. If the secondary antibody had bound to proteins in the control, then the brighter fluorescence observed in Figures 1, 3, and 7 would also appear in Figures 5 and 9. The presence of cytokeratins in the zebrafish optic nerve is supported by previous research (García et al. 2005, Cohen et al. 1993). Further research concerning cytokeratins in the zebrafish optic nerve could concern identification of the cells expressing the IF, as well as further clarification the structure of the keratin found in the optic nerve.

The dullness observed in the GFAP control sections (Figures 13 and 17) indicates there was little or no secondary antibody binding in the absence of the primary antibody. The intense labeling of Müller glia projections in the retina observed in Figure 15 indicates that the anti-GFAP antibody is labeling GFAP, but there is too much non-specific labeling in these sections to determine conclusively that GFAP is expressed in zebrafish optic nerve. Purified monoclonal mouse anti-GFAP should be specific for GFAP, and only GFAP. The intense labeling observed in Figure 11 should be indicative of GFAP. However, there is

labeling in tissues where GFAP is not found. Muscle tissue, for instance, does not contain GFAP. Nor do blood vessels, which can be observed in Figure 11. There are several reasonable explanations for this discrepancy. The concentration of primary antibody may have caused non-specific binding. A lower concentration may demonstrate more specific binding. The blocking agent used may not have been strong enough; in which case, using a more concentrated blocking agent would produce more specific binding. There have been instances of anti-GFAP antibody binding to tissues not associated with GFAP, including muscle (Albrechtson, et al. 1984). The non-specific binding of anti-GFAP antibodies could be attributed to the similarities of GFAP to other type III IFs, such as vimentin and desmin. IF types are designated according to their similar amino acid sequences, and vimentin, desmin, and GFAP are all type III IFs (García et al., 2005). The labeling observed in the experimental GFAP sections (Figure 13) could be due to anti-GFAP binding to vimentin and desmin, which are found in the fish visual pathway (Cohen et al. 1993) and muscle tissue (Kim and Coulombe., 2007), respectively. Vimentin is the IF found most prevalently in the visual pathway of fish, including the optic nerve (Nona et al., 1989). Thus, the labeling in the optic nerve observed in Figure 11 could be due to the presence of GFAP, vimentin, or another type III IF. This labeling therefore cannot be considered evidence that GFAP is expressed in the zebrafish optic nerve. The labeling does not confirm the presence of GFAP in the optic nerve, but it also does not deny the presence of the IF. The labeling may very well be due to the presence of GFAP, but because it is unclear what other IFs are being labeled with the antibody, the type being labeled in the optic nerve cannot be determined.

Further experimentation with different concentrations of antibody and blocking agent, or a different anti-GFAP antibody altogether, could further clarify the location of GFAP in

zebrafish optic nerve. Using anti-vimentin and anti-desmin antibodies could also indicate what other IFs the primary antibody is binding to. Research concerning the IFs found in the zebrafish visual pathway will continue, and will contribute to determining the type and structure of cells found there.

REFERENCES

Aebi, U, M Haner, J Troncoso, R Eichner, and A Engel. 1988. Unifying principles in intermediate filament (IF) structure and assembly. *Protoplasma* 145:73-81.

Alberts, B. A Johnson, J Lewis, M Raff, K Roberts, and P Walter. 2007. Intermediate filaments. *Molecular Biology of the Cell, 5th Ed*. Garland Science Group, NY.

Albrechtsen, M., A C von Gerstenberg, and E Bock. 1984. Mouse monoclonal antibodies reacting with human brain glial fibrillary acidic protein. *Neurochem* 42: 86-93.

Cohen, I, Y Shani, and M Schwartz. 1993. Cloning and characteristics of fish glial fibrillary acidic protein: implication for optic nerve regeneration. *J Comp Neuro* 334:431-443.

Erber, A, D Reimer, M Bovenschulte, and K Weber. 1998. Molecular phylogeny of metazoan intermediate filament proteins. *J Mol Evol* 47:751-762.

García, DM, H Bauer, T Dietz, T Shubert, J Markl, and M Schaffeld. 2005. Identification of keratins and analysis of their expression in carp and goldfish: comparison with the zebrafish and trout keratin catalog. *Cell Tissue Res* 322:245-256.

García, DM and JR Koke. 2009. Astrocytes as gate-keepers in optic nerve regeneration—a mini-review. *Comp Biochem and Physiol* 152:135-138.

Goldman, RD, S Khuon, YH Chou, P Opal, and PM Steinert. 1996. The function of intermediate filaments in cell shape and cytoskeletal integrity. *J Cell Biol* 134:971-983.

Herrmann, H and JR Harris. 1998. Cyprinid teleosts: goldfish optic nerve, carp, and zebrafish tissues. *Intermediate Filaments*. Plenum Publishing, New York, NY.

Kawai, H, N Arata, and H Nakayasu. 2001. Three-dimensional distribution of astrocytes in zebrafish spinal cord. *Glia* 36:406-413.

Kim, Seyun and PA Coulombe. 2007. Intermediate filament scaffolds fulfill mechanical, organizational, and signaling functions in the cytoplasm. *Genes and Devel* 21: 1581-1597.

Krushna, PB, MA Akimenko, and M Ekker. 2006. Independent expansion of the keratin gene family in teleostean fish an mammals: an insight from phylogenetic analysis and radiation hybrid mapping of keratin genes in zebrafish. *Gene* 368: 37-45.

Lipman, NS, LR Jackson, LJ Trudel, and F Weis-García. 2005. Monoclonal versus polyclonal antibodies: distinguishing characteristics, applications, and information resources. *ILAR* 46(3).

Maeyama, K and H Nakayasu. 2000. Postembryonic neurogenesis in zebrafish (*Danio rerio*) brain: presence of two different systems. *Zool Sci* 17:285-294.

Menet, V, MGY Ribotta, F Sandillon, and A Privat. 2000. GFAP null astrocytes are a favorable substrate for neuronal survival and neurite growth. *Glia* 31:267-272.

Nona, SN, SAS Shehab, CA Stafford, and JR Cronly-Dillon. 1989. Glial fibrillary acidic protein (GFAP) from goldfish: its localization in visual pathway. *Glia* 2:189-200.

Parry, DAD and PM Steinert. 1999. Intermediate filaments: molecular architecture, assembly, dynamics and polymorphism. *Q Rev Biophys.* 32:99-187.

Sokolova, AV, L Kreplak, T Wedig, N Mucke, DI Svergun, H Herrman, U Aebi, and SV Strelkov. 2006. Monitoring intermediate filament assembly by small-angle x-ray scattering reveals the molecular architecture of assembly intermediates. *Proc Nat Academ Sci USA* 44: 16206-16211.

Strelkov, SV, H Herrmann, N Geisler, T Wedig, R Zimblemann, U Aebi, and P Burkhard. 2002. Conserved segments 1A and 2B of the intermediate filament dimmer: their atomic structures and role in filament assembly. *EMBO J* 21:1255-1266.